
MACHINE LEARNING BASED INDICATORS TO ENHANCE PROCESS MONITORING BY PATTERN RECOGNITION

A PREPRINT

Stefan Schrunner
Department of Data Science
Norwegian Univ. of Life Sciences
Ås, Norway
stefan.schranner@nmbu.no

Michael Scheiber
KAI GmbH
Villach, Austria
michael.scheiber@k-ai.at

Anna Jenul
Department of Data Science
Norwegian Univ. of Life Sciences
Ås, Norway
anna.jenul@nmbu.no

Anja Zernig
KAI GmbH
Villach, Austria
anja.zernig@k-ai.at

Andre Kaestner
Infineon Technologies Austria AG
Villach, Austria
andre.kaestner@infineon.com

Roman Kern
Know-Center GmbH
Graz University of Technology
Graz, Austria
rkern@know-center.at

September 9, 2022

ABSTRACT

In industrial manufacturing, modern high-tech equipment delivers an increasing volume of data, which exceeds the capacities of human observers. Complex data formats like images make the detection of critical events difficult and require pattern recognition, which is beyond the scope of state-of-the-art process monitoring systems. Approaches that bridge the gap between conventional statistical tools and novel machine learning (ML) algorithms are required, but insufficiently studied. We propose a novel framework for ML based indicators combining both concepts by two components: pattern type and intensity. Conventional tools implement the intensity component, while the pattern type accounts for error modes and tailors the indicator to the production environment. In a case-study from semiconductor industry, our framework goes beyond conventional process control and achieves high quality experimental results. Thus, the suggested concept contributes to the integration of ML in real-world process monitoring problems and paves the way to automated decision support in manufacturing.

Keywords Process monitoring · critical events · error detection · pattern recognition · machine learning based indicator

This work has been submitted to the IEEE for possible publication. Copyright may be transferred without notice, after which this version may no longer be accessible.

1 Introduction

Across all industries, manufacturing processes require permanent monitoring to guarantee consistent high quality of products. Industry 4.0 demands even more extensive control since systems operate autonomously. At the same time, larger and more complex datasets are produced. Since human observers cannot monitor the systems anymore, not only production but also process monitoring requires novel concepts.

Statistical process control was coined by Shewhart [1] nearly 100 years ago, followed by contributions from different areas in statistics and mathematics. In the last decades, machine learning (ML) techniques have become part of real-world applications and opened for new possibilities in this area — yet, integrating ML methods into the existing systems is not trivial, since both concepts have fundamental differences. An important state-of-the-art tool in process monitoring is the control chart, where control limits are specified for a parameter under investigation in order to detect

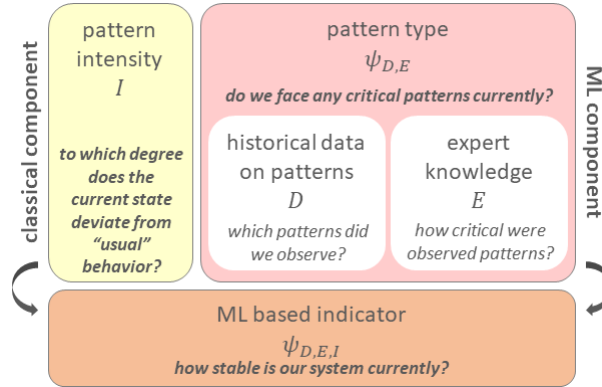


Figure 1: Components of the presented framework of ML based indicators for process monitoring.

critical events (significant deviations) in the process. Since univariate control chart concepts are not sufficient in many cases, multivariate extensions exist, involving statistical tools like Partial Least Squares (PLS) and Principal Component Analysis (PCA). An exhaustive overview of this field is provided by Bersimis et al. [2]. Recent research works present alternative approaches to deal with multivariate settings: Liu et al. [3] propose a monitoring framework for industrial processes with multiple operational conditions, which combines probabilistic linear discriminant analysis with an expectation maximization algorithm. Still, these approaches have only limited capability of integrating general ML algorithms for recognizing error patterns in process data. In particular, the ability to cover data formats and structures produced by manufacturing equipments in Industry 4.0 is limited. While conventional process monitoring is specialized on tracking error modes in few key parameters, modern manufacturing environments deliver more complex data formats (time series, image data), instead. This aspect brings up the idea to integrate ML for recognition of error patterns to a larger extent.

Multiple research works directly adapt ML algorithms for reasoning-based diagnosis. Jin et al. [4] describe a diagnosis system which can be applied to decision trees, support vector machines, neural networks as well as Naive Bayes classifier. Ge and Song [5] apply unsupervised dimensionality reduction by an adaptive variant of PCA to monitor semiconductor production processes. Yu [6] elaborated on Gaussian Mixture Models for a similar purpose, resolving some of the limitations of PCA. A survey on unsupervised approaches is provided by Aldrich and Auret [7], while supervised ML approaches are summarized by Wuest et al. [8] and Lv et al. [9]. Furthermore, Angelopoulos et al. [10] present a thorough survey on recent ML solutions in Industry 4.0 applications, covering a broad palette of different subject areas like cloud architectures, fault detection, predictive maintenance, human machine interaction, security and threat detection and many more. Although the mentioned research works already exploit ML methods, none of them analyzes how the information extracted by ML fits to classical approaches in a mathematically rigorous way by a generalizable framework. To ensure a smooth extension from classical process monitoring to modern pattern recognition systems in industry, it is crucial that the new indicators fit the interfaces of previously implemented systems. Thus, a novel framework is required to bridge the gap between the classical and ML approaches. Using the generic framework proposed in this work, it is possible to design process monitoring systems based on ML, such that the required consistency is preserved.

Our main contribution is to define a novel framework of generic conditions, which ensure the compatibility of an ML based indicator for process monitoring with the established manufacturing environment. Therefore, we propose two independent model components summarized in Fig. 1:

1. the type of a detected failure pattern (type of event indicating the criticality of its associated failure mode),
2. the intensity of the pattern (degree of deviation indicated by the event).

Further we argue that classical indicators like control charts are a special case of the presented concept. To demonstrate the real-world use, we present a case study from semiconductor industry, where the detection of process patterns is performed using methods from image processing and ML in analog wafer test data. This approach goes beyond the assessment of classical pass/fail test investigations of semiconductor products and thus, is optimally suited for demonstrating the capabilities of the concept. In an experimental evaluation, we underline the ability of the novel concept to involve previously unused aspects like recognition of the error pattern.

2 ML based indicators for process monitoring

The framework we propose defines mathematical requirements of a valid ML based indicator for process monitoring. In this context, an indicator ψ is a function $\psi : \mathcal{D} \rightarrow \mathbb{R}$, which assigns a level of concern, risk or loss to any data point d (a parameter, a time series, an image or similar) in an according domain \mathcal{D} . From a mathematical perspective, (\mathcal{D}, m) is a pseudometric space with a distance measure $m : \mathcal{D} \times \mathcal{D} \rightarrow \mathbb{R}^+$ describing the mutual dissimilarity between objects in \mathcal{D} . A pseudometric m is a mapping to the positive real numbers, which fulfills the following conditions:

$$m(x, x) = 0, \forall x \in \mathcal{D}, \quad (1)$$

$$m(x, y) = m(y, x), \forall x, y \in \mathcal{D}, \quad (2)$$

$$m(x, z) \leq m(x, y) + m(y, z), \forall x, y, z \in \mathcal{D}. \quad (3)$$

Thus, a pseudometric prevents contradictions and guarantees faster computation due to the triangle equation, Eq. 3. In contrast to a full metric, Eq. 1 does not require that $x = y$, if $m(x, y) = 0$.

We assume that a set of historical data is available, given by $D \subset \mathcal{D}$. In addition, expert knowledge $E : D \rightarrow [0, 1]$ is present for these data points. The latter assumption conveys that experts are able to judge situations, which occurred in the past, due to their experience and insight into the process. The goal of the ML based indicator is to generalize the knowledge obtained from D to the whole data domain \mathcal{D} in order to cover future outcomes. An indicator ψ bundling information from D and E is denoted by $\psi_{D,E}$, as indicated by the pattern type block in Fig. 1.

2.1 Definition of an ML based indicator

An ML based indicator for process monitoring needs to comply with intuition, as well as with practical requirements. Two fundamental properties are:

1. non-negativity:

$$\psi_{D,E}(x) \geq 0, \quad (4)$$

for any $x \in \mathcal{D}$ — hence, the indicator exclusively provides values greater than or equal to 0. In detail, we denote uncritical states by 0, while increasingly high values indicate a higher risk for the presence of critical events. Moreover, since the indicator maps to the set of real numbers, it can be assumed to deliver interval-scaled data, which is required for the second condition. In many cases, it is additionally reasonable, but not mandatory to require that $\psi_{D,E} \in [0, 1]$, so that the indicator is bounded. Bounded data scales facilitate the definition of thresholds to trigger warnings or alerts.

2. consistency:

$$|\psi_{D,E}(x) - E(d)| \leq \alpha \cdot m(x, d) + \beta, \quad (5)$$

for any $x \in \mathcal{D}$, and $d \in D$ within a local neighborhood $m(x, d) \leq m_{\max}$, $m_{\max} > 0$. Here, $\alpha, \beta > 0$ are constants, where β is assigned to a small value. In other words, for any $x \in \mathcal{D}$ obtained from the process, a similar value as for the historical point $d \in D$ should be obtained, if the data point x is close to d (with respect to m). This property implies that $\psi_{D,E}(x) \approx E(d)$, if $m(x, d) \rightarrow 0$. The value of β judges the variation of the indicator in neighborhoods around historical points. The condition delivers smoothness around points assessed by the expert.

In general, probabilistic systems are not able to meet the condition of consistency exactly, thus we require that it holds for most (instead of all) $x \in \mathcal{D}$, allowing few violations of the criterion. This leads to the **relaxed consistency** condition

$$P(|\psi_{D,E}(x) - E(d)| \leq \alpha \cdot m(x, d) + \beta) \geq 1 - \xi, \quad (6)$$

where P denotes the underlying probability measure and $\xi > 0$ is a probability slightly greater than 0. Both consistency and relaxed consistency restrict the m_{\max} -neighborhood around historically classified points, while previously unseen areas remain unaffected. As a consequence of the stated definition, an indicator $\psi_{D,E}$ will conform with the expert knowledge provided by E ,

$$\psi_{D,E}(d) = E(d) \pm \beta, \quad (7)$$

for $d \in D$ and small $\beta > 0$, or alternatively $\psi_{D,E}|_D \approx E$. This condition delivers consistency with the expert knowledge: for $d \in D$, it follows from $m(d, d) = 0$ that

$$|\psi_{D,E}(d) - E(d)| \leq \beta. \quad (8)$$

To connect $\psi_{D,E}$ with common ML frameworks, we investigate how a pseudometric m can be defined in clustering and classification problems: Many ML algorithms are based on proper metrics as distance measures, which delivers an

intuitive choice for the pseudometric of $\psi_{D,E}$. For instance, prototype-based clustering algorithms, such as k-means, characterize clusters by centroids, which represent the center point of the cluster with respect to a given distance measure, such as the Euclidean distance. Similarly, k-nearest neighbor classifiers assign the label of their nearest neighbors in the feature space to new objects — in both cases, distance measures reflect the degree of membership to the according cluster or class. Also in density-based clustering, a metric is required to define high- and low-density regions. In many cases, such distance measures fulfill the conditions of a pseudometric and can be used for m in a direct way. Exceptions include, for instance, the cosine similarity measure, which violates the triangle equation.

In cases where no suitable distance measure is delivered by the classification or clustering algorithm, a pseudometric m can be obtained from the predicted class (cluster) memberships. If probabilistic approaches are used, the according class (cluster) membership probability represents a suitable choice for m . Otherwise, a coarse pseudometric is induced by hard class (cluster) memberships $c(\cdot)$ of points $x, y \in \mathcal{D}$:

$$m(x, y) := \begin{cases} 0 & c(x) = c(y), \\ 1 & \text{else.} \end{cases} \quad (9)$$

2.2 Enhancing the concept by intensity

Based on the definition of an ML based indicator $\psi_{D,E}$, the concept shall be extended to cover all information, which is relevant to assess a state of the process. In many cases, both intrinsic and extrinsic information (information from the data and information not contained in the data, respectively) are available to assess the level of concern associated with a data point — the concept defined above covers the extrinsic part by extrapolating knowledge from the expert. Intrinsic information covers the intensity of a state, defined as the deviation from the "average" instances of the process. In contrast to the extrinsic information from the expert, intrinsic information is acquired objectively and without explicit domain knowledge, for instance by calculating the difference between the current state and an average over historical data. We refer to extrinsic information as criticality associated with a pattern type, while we denote intrinsic information as intensity. ML can be used for both aspects: while criticality implies typical supervised learning scenario, intensity describes an unsupervised aspect.

To include intensity into the generic concept, we extend the framework: we introduce a measure $I : \mathcal{D} \rightarrow [0, 1]$, which implements the suggested intensity concept — 0 denotes an average state and 1 denotes a strong deviation from the average. The final indicator, unifying the concepts of intensity and criticality, is then denoted by $\psi_{D,E,I} : \mathcal{D} \rightarrow \mathbb{R}$, where $\psi_{D,E,I}(x) = \varphi(\psi_{D,E}(x), I(x))$ for a predefined, monotonic functional φ , by default $\varphi(f_1, f_2)(x) = f_1(x) \cdot f_2(x)$. While the non-negativity assumption remains unchanged, the consistency assumption must be extended by

$$|\psi_{D,E,I}(x) - \varphi(E(d), I(d))| \leq \alpha_1 \cdot m(x, d) + \alpha_2 \cdot |I(x) - I(d)| + \beta, \quad (10)$$

for small constants $\alpha_1, \alpha_2 > 0$. Hence, the value of the indicator is dependent on both, the intensity and the distance in the feature space between two states. In other words, if a data point x is close to d and both have similar intensity values, $I(x) \approx I(d)$, then the indicator should provide similar values. In contrast, the values of $\psi_{D,E,I}(x)$ and $E(d)$ may be significantly different, if either the distance between x and d is large (distinct pattern types), or the intensity of both points is different (distinct degree of development).

2.3 Control chart as special case of ML based indicators

Control charts are a prominent method in process monitoring and a major tool of quality control, intended to detect whether processes are stable or not. A univariate control chart is used to demonstrate how the suggested conditions are fulfilled in a classical process monitoring setup. Implicitly assuming a normal distribution of the single process variables under investigation, the control limits are calculated from robust moments of the data distribution to reduce the impact of outliers. In specific, a given test parameter s is measured over a time period T , delivering the time series $\{s_t, t \in T\}$. We observe a historical period from the time series $D = \{s_t, t \in T_D\}$, $T_D \subset T$, which delivers a parameter estimate for the model:

$$\hat{\mu}_{robust} = Q_{0.5}((s_t)_{t \in T_D}), \quad (11)$$

$$\hat{\sigma}_{robust} = \frac{Q_{(1-k)}((s_t)_{t \in T_D}) - Q_k((s_t)_{t \in T_D})}{2\gamma}, \quad (12)$$

where $Q_\tau(\cdot)$ denotes the empirical τ -quantile of $\{s_t, t \in T_D\}$ (ignoring the time dependence), $k \in (0, 0.5)$ is a small constant and $\gamma \in \mathbb{R}^+$ is a normalizing factor. A common choice is $k = 0.25$, delivering the Inter-Quartile-Range with

associated $\gamma = 0.674$. In statistical process control, so-called lower and upper control limits (LCL and UCL) are defined based on these parameters as

$$LCL = \hat{\mu}_{robust} - \ell \cdot \hat{\sigma}_{robust}, \quad (13)$$

$$UCL = \hat{\mu}_{robust} + \ell \cdot \hat{\sigma}_{robust} \quad (14)$$

with $\ell > 0$. A prominent choice in semiconductor industry is to set limits with $\ell = 6$, denoted as *Part Average Testing* (PAT) [11].

In the light of the discussed framework of ML based indicators, the procedure of thresholding the values s_t with LCL and UCL can be interpreted as intensity measure

$$i(s_t) = \begin{cases} 0 & s_t \in [LCL, UCL], \\ 1 & \text{else.} \end{cases} \quad (15)$$

Since control limits do not discriminate between different types of deviations, all instances $s_t, t \in T$ are assumed to represent the same pattern type $p \in \mathcal{P}$, $c(s_t) \equiv p$, and hence $\psi_{D,E}(s_t) \equiv E(s_t) \equiv 1$ and $\psi_{D,E,I}(s_t) = i(s_t)$. The resulting indicator $\psi_{D,E,I}(s_t)$ returns positive values and thus, fulfills the non-negativity condition. With regard to consistency, $m(x, d)$ is obviously equal to 0. The consistency property reads

$$|\psi_{D,E,i}(s_{t_1}) - E(s_{t_2}) \cdot i(s_{t_2})| \leq \alpha_2 \cdot |i(s_{t_1}) - i(s_{t_2})| + \beta, \quad (16)$$

for $t_1 \in T$ and $t_2 \in T_D$. According to the definition of $\psi_{D,E,I}$ and the property that $E \equiv 1$, this is equivalent to

$$|i(s_{t_1}) - i(s_{t_2})| \leq \alpha_2 \cdot |i(s_{t_1}) - i(s_{t_2})| + \beta. \quad (17)$$

This condition is satisfied for any $i(s_{t_1}), i(s_{t_2}) \in \{0, 1\}$, for example by setting $\alpha_2 = 1$. Hence, ordinary control charts including PAT satisfy our definition of an ML based indicator. Analogously, also multivariate variants of control charts fulfill the conditions of non-negativity and consistency. Hence, our work directly extends classical approaches in process monitoring — however, the flexibility of the concept goes beyond standard examples, as will be demonstrated in a more complex application.

3 A Case Study from Semiconductor Industry

In semiconductor industry, like in many other advanced manufacturing domains, a common problem is to judge the stability of the production process and distinguish between critical and uncritical types of events — while critical events can lead to violations of product specifications, uncritical events have no impact on product quality. The production process consists of hundreds of synchronized process steps with limited possibilities to conduct functional in-line measurements. As a rule, the quality of the product can only be judged at the end of (frontend) wafer production, the wafer test stage. Here, electrical parameters are measured for each device on the wafer, testing major functional aspects of the product. When analyzing these measurement data and considering the spatial positions of the devices on the wafer, characteristic patterns can be obtained and traced back to events like process deviations. In particular, the problem shows the following challenges:

- each observed instance is a heatmap (wafermap) of a whole wafer, comparable to a grayscale image, instead of a single data point,
- critical states need to be detected by pattern recognition on wafermaps rather than by univariate operations delivering single key values,
- a large variety of patterns exists, where some depict critical events, while others are unimportant for process monitoring (such as patterns evoked by the testing procedure itself).

To a large extent, state-of-the-art process monitoring in semiconductor manufacturing is based on techniques like yield loss or dynamical PAT: Yield loss is the simplest approach, where the ratio of devices per wafer violating specification limits in the wafer test procedure is taken as a quality indicator. Dynamical PAT is a specific version of PAT, where control limits are based on robust empirical quantiles to identify and remove outliers from the tested devices within the specification range. Both methods, yield loss and PAT, are not able to cover the complexity of the problem: they neither take spatial positions into account, nor discriminate between critical and uncritical pattern types. Hence, a more comprehensive ML based indicator is required: we evaluate the Health Factor for Process Patterns, introduced by Schrunner et al. [12].¹

¹A distinct concept named *Health Factor* exists for predictive maintenance [13], but is unrelated to the Health Factor discussed in this work.

3.1 Definition of the Health Factor

The Health Factor consists of three components: pattern type, associated pattern (type) criticality, and pattern intensity. The pattern type results from a pattern recognition algorithm, which analyzes the spatial dependencies between devices and assigns each wafermap to a specific class of process patterns. According to expert knowledge, each pattern type (class) is evaluated with respect to criticality, a level of potential quality concern associated with the occurrence of the pattern. Upon multiple wafermap classification approaches available in recent works [14–17], we deploy the pipeline suggested in [12], which operates on analog wafermaps and consists of preprocessing via Markov Random Fields to remove noise and background structures, a feature extraction step and a subsequent selection of classification method. As image features, a combination of Local Binary Pattern (LBP), Rotated Local Binary Pattern (RLBP) feature selectors (adapted for this purpose by Santos et al. [18]) and Histogram of Oriented Gradients (HOG) [19] is used — however, a broad range of further feature selectors are available in literature [20–22]. Using this set of features the invariance properties of patterns, invariance with respect to scale, rotation and position, can be taken into account. After transformation into a feature space \mathcal{F} , the pattern type $p_w \in \mathcal{P}$ of a wafermap $w \in \mathcal{F}$ can be predicted by a classifier $c : \mathcal{F} \rightarrow \mathcal{P}$, such that (in case of a correct classification) $c(w) = p_w$. Here, \mathcal{P} is a set of distinct pattern types (classes) specified by labeled training data. Using expert knowledge, each pattern type is mapped to a criticality value $h(p)$ in the interval $[0, 1]$, where 0 denotes uncritical pattern types and 1 denotes critical ones.

Independently, the concept of intensity is required since each pattern type can be observed at different degrees of development (ranging from weak to very strong states). In a weak state, a pattern slightly deviates from measurement noise, while in a strong state, measured values are large and scratch the specification limits or affect a large region on the wafermap. Note that the concept does not overlap with pattern type classification: while pattern type classification is targeted on the shape and position of the pattern on the wafermap, intensity describes the degree of development within a pattern type (class). The intensity concept is implemented via statistical autocorrelation methods, as suggested in [23]. Especially the Moran’s I [24], a direct generalization of the autocorrelation defined for stochastic processes, proved to be useful. In the following, we denote $i(w)$ as the Moran’s I value of the wafermap $w \in \mathcal{F}$.

The three components p , h and i are combined using statistical decision theory: the loss function, which determines the outcome of a decision given a pattern type, is defined as $L(w, p) = i(w) \cdot h(p)$. The Bayesian risk averages the loss over all possible pattern types: as expected value of the loss function with respect to the probability distribution P , it judges the level of uncertainty associated with the underlying state of nature, as well as the impact of the potential outcome. Related to Fig. 1, the Health Factor HF_w , which delivers the structure of an ML based indicator according to Section 2, is given by

$$\underbrace{HF_w}_{\psi_{D,E,I}} = \underbrace{i(w)}_I \cdot \underbrace{\sum_{p \in \mathcal{P}} h(p) \cdot P(c(w) = p)}_{\psi_{D,E}}. \quad (18)$$

While non-negativity condition is trivially met by HF_w , consistency must be observed in detail: Expert knowledge $E(d)$ is available on level of the pattern types c_i , given by $E(d) = E(c(d))$, where $c(\cdot)$ is the ground truth class assignment of the training data point $d \in D$. Furthermore, the pseudometric m is defined as specified in Eq. 9:

$$m(x, y) := \begin{cases} 0 & c(x) = c(y) \\ 1 & \text{else.} \end{cases}$$

Given that two data points $d \in D$ and $x \in \mathcal{D}$ are located in a spatial neighborhood to each other with respect to m , $m(x, d) < m_{\max}$, $0 < m_{\max} < 1$, these elements will be assigned to the same class by the classifier c due to the smoothness assumption underlying the applicable ML algorithms. Since the criticality $h(\cdot)$ is judged per pattern type, the same value is obviously assigned to elements x and d , such that $\psi_{D,E}(x) = \psi_{D,E}(d)$. Since a classifier is trained to approximate an optimal ground truth class assignment $c^* : w \rightarrow p_w \in \mathcal{P}$ by a generative or discriminative model, it is assured that the criterion $\psi_{D,E}(d) = E(d)$ holds in a large majority of cases. Since the classifier cannot deliver a 100% accuracy, it may occur that $c(w) \neq p_w$ — nevertheless, the relaxed consistency criterion remains unaffected from such rare events.

3.2 Experimental setup

The applicability of the Health Factor is assessed on 3 real-world datasets with different characteristics:

- a) *dataset*₁: A simulated dataset showing 5 different pattern types (1-5), comprising 400 wafermaps from each out of 5 pattern types, resulting in 2,000 wafermaps in total.²

²The dataset is available at <http://www.doi.org/10.5281/zenodo.2542504>.

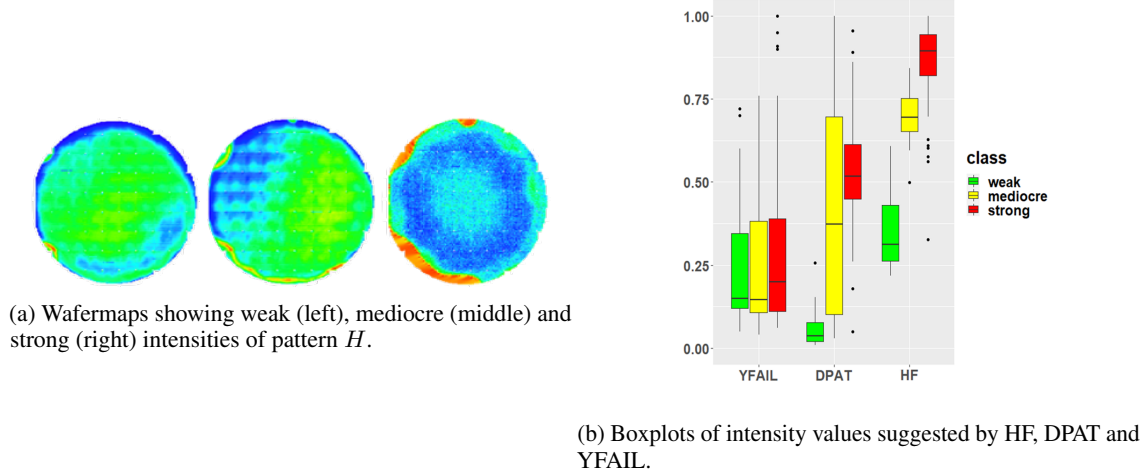


Figure 2: Sample wafermaps showing a critical pattern at different intensity levels, and intensity quantification results from yield loss (YFAIL), dynamical PAT (DPAT) and Health Factor (HF). Coloring of the boxplots represents expert judgment.

- b) $dataset_2$: 4,324 wafermaps from a real-world product showing 8 different pattern types ($A-H$). The dataset is unbalanced due to different occurrence frequencies between types of critical events in the underlying process.
- c) $dataset_3$: A dataset of a distinct semiconductor product, containing 679 wafermaps with 4 different pattern types ($\mathfrak{A}-\mathfrak{D}$).

In order to evaluate the Health Factor and its components, one or more critical pattern types are specified by domain experts in each of the 3 datasets. The vectors assigning criticality values to each pattern type in $dataset_1$, $dataset_2$ and $dataset_3$ are denoted by h_1 , h_2 and h_3 , respectively. For the simulated dataset $dataset_1$, the criticality is set to $h_1(1) = 1, h_1(2) = h_1(4) = 0.5, h_1(3) = h_1(5) = 0$. For $dataset_2$ the critical pattern type is H , while for $dataset_3$, pattern type \mathfrak{A} is critical, such that $h_2(H) = 1$ and $h_3(\mathfrak{A}) = 1$. All other pattern types get assigned criticality 0.

The evaluation procedure is conducted in 3 distinct setups:

- a) evaluation of the pattern intensity concept, compared with state-of-the-art concepts yield loss and dynamical PAT (control charts),
- b) evaluation of the pattern type classification concept,
- c) evaluation of the Health Factor thresholds.

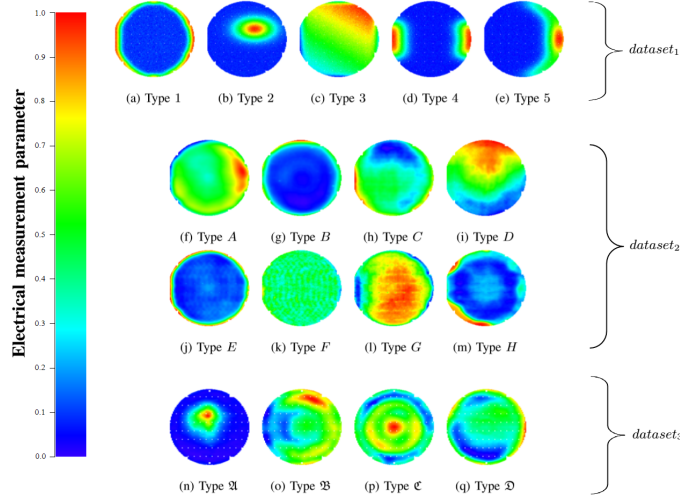
Each setup is repeated 100 times on each dataset, providing a summary statistic of the results in order to assure consistency and average out the influence of good or bad runs. In each run, train and test subsets are sampled in a balanced way: the train-test-splits of $dataset_1$ consist of 100 wafermaps (per pattern type) in the training and 100 wafermaps (per pattern type) in the test set (100/100). In $dataset_2$, a train-test-split of 100/147 and in $dataset_3$, a train-test-split of 40/45 is chosen.

3.3 Results

First, we perform an evaluation with focus on intensity variation within a (known) critical pattern class of $dataset_2$ — this aspect is a direct extension to concepts like yield loss and PAT. Therefore, we leave the classification component out and restrict to the subset of wafermaps from $dataset_2$, which are assigned to pattern type H (a total number of 170 wafermaps). These wafermaps are manually classified into 3 categories representing the degree of development of the pattern, demonstrated in Fig. 2a:

- weak (73 wafermaps): slight contours of the pattern,
- mediocre (20 wafermaps): contours visible, but with low contrast,
- strong (77 wafermaps): clear contours over the wafermap.

We analyze the Health Factor (HF), dynamical PAT (DPAT) and yield loss (YFAIL) values delivered for each wafermap with respect to these ground truth categories. Results for all combinations are presented as boxplots in Fig. 2b: HF



(a) Example wafermaps of pattern types: wafermaps (a)-(e) correspond to $dataset_1$, wafermaps (f)-(m) to $dataset_2$ and wafermaps (n)-(q) to $dataset_3$. The values range from low (blue) to high (red).

		F1 score					
Pattern Type		total	NB	RF	SVM_l	SVM_p	LR
$dataset_1$	1	400	1.000	1.000	1.000	0.867	1.000
	2	400	0.994	1.000	0.964	0.775	0.999
	3	400	1.000	1.000	1.000	0.978	1.000
	4	400	1.000	1.000	0.981	0.794	0.999
	5	400	0.994	1.000	0.984	0.959	1.000
	average		0.997	1.000	0.986	0.874	1.000
$dataset_2$	A	568	0.998	1.000	1.000	0.933	0.999
	B	566	0.994	0.994	0.965	0.728	0.997
	C	918	0.868	0.997	0.943	0.403	0.998
	D	568	0.981	0.990	0.969	0.788	0.994
	E	284	1.000	1.000	0.997	0.990	1.000
	F	852	0.975	0.995	0.979	0.956	0.996
	G	284	0.979	0.993	0.959	0.807	0.993
	H	284	0.807	0.990	0.910	0.675	0.997
	average		0.950	0.995	0.965	0.785	0.997
$dataset_3$	Ⓐ	194	0.998	1.000	1.000	0.991	0.932
	Ⓑ	194	0.935	0.970	0.870	0.709	0.879
	Ⓒ	194	0.922	0.965	0.873	0.783	0.864
	Ⓓ	97	0.976	0.986	0.954	0.921	0.900
		average		0.958	0.980	0.924	0.851

(b) Macro-averaged F1 scores for each dataset, pattern type and classifier.

Figure 3: Experimental data and pattern type classification results on 3 datasets.

discriminates well between all three categories with few outliers. DPAT values differ between weak and mediocre/strong wafermaps, while mediocre and strong wafermaps cannot be distinguished. YFAIL cannot cover distinct intensity levels accurately, which might be caused by the aggregation of multiple error modes, while DPAT and HF assess wafermaps individually.

To enhance the analysis with quantitative results, a one-way analysis of variance (ANOVA) is performed, evaluating the evidence for class differences between classes weak, mediocre and strong. ANOVA is performed with respect to each of the three indicators HF, DPAT and YFAIL, separately. The analysis consists of an F -test to investigate whether or not class differences exist, followed by a pairwise t -test to identify the affected class pairs, if indicated. YFAIL provides no evidence to reject the null hypothesis H_0 , suggesting that all classes are equal (p-value $> 8 \cdot 10^{-1}$). In contrast, HF and DPAT clearly reject H_0 (p-value $< 2 \cdot 10^{-16}$ and $< 2 \cdot 10^{-12}$, respectively). The pairwise t -test with Tukey correction for simultaneous testing confirms that HF values significantly differ between all pairs of classes (all p-values $< 10^{-6}$). DPAT is likewise suited to distinguish between weak and strong (p-value $< 10^{-16}$), as well as between weak and mediocre wafermaps (p-values $< 10^{-5}$), whereas the p-value of the comparison between classes mediocre and strong is in a marginal range (p-value $4 \cdot 10^{-2}$). Hence, ANOVA supports the observation that HF is better suited to discriminate between mediocre and strong patterns on wafermaps, while weak patterns can be detected by DPAT with similar performance. YFAIL does not provide an accurate indication for class differences.

In the previous experiment, the full power of ML concepts was not yet exploited, since no distinction between pattern types was made. Hence, we introduce pattern type classification using a selection of 5 classification methods:

- a) Naive Bayes classifier (NB)
- b) Random Forest (RF)
- c) Support Vector Machine with linear kernel (SVM_l)
- d) Support Vector Machine with polynomial kernel (SVM_p)
- e) Logistic Regression with one-vs-one classification (LR)

Classification quality is evaluated via F1 scores, representing the harmonic mean of precision and recall for each of the different pattern types. In order to address the multi-class problem, the F1 score is averaged over all classes (macro-averaging). Fig. 3 presents sample wafermaps from all classes, along with calculated F1 scores for each dataset, pattern type and classification method. All classifiers yield accurate results, underlining that the set of features covers all necessary information to model the pattern type. With the exception of SVM_p , all classification methods achieve an F1 score of at least 0.90 for all 3 datasets. RF classification yields the best results with an average F1 score of at least 0.98. On the other hand, LR seems to outperform the RF for larger datasets.

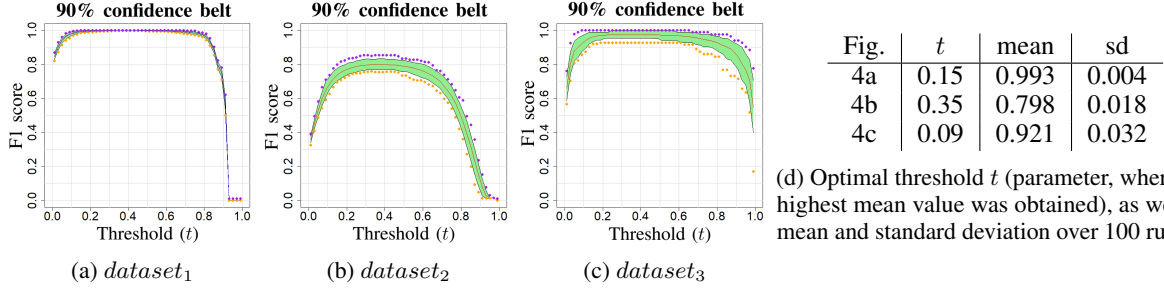


Figure 4: 90% confidence belts of averaged F1 scores for each dataset of the F1 score depending on the chosen threshold. Minimum and maximum values per threshold are indicated as purple and orange dots, respectively.

As final experiment, we evaluate the full concept of the HF at once. For this purpose, we use a ground truth for the predicted HF values, where the expert assigns a 0-1 coding to each wafermap, quantifying whether the wafermap depicts a critical pattern, which should trigger an alarm. During evaluation, the HF value is thresholded by a value t and set to 1, if the indicator value is above the threshold t and 0, else. F1 scores are calculated for each dataset when comparing the ground truth 0-1-coding by the expert to the 0-1-coding obtained from the HF. Hence, a low threshold t results in predicting many wafermaps as 1 and obtaining a low precision, while a high threshold yields many 0-predictions and a low recall. Classification is based on RF due to its superior overall performance in the previous experiment. Fig. 4 shows the resulting F1 scores averaged over 100 runs, along with 90% confidence belts, as function of t . Among all datasets, the confidence belts indicate that the F1 scores are robust with respect to the selection of the threshold t , which is relevant for practical applications. Throughout the high F1 scores indicating stable and accurate results, the maximum F1 score for *dataset₂* of approx. 0.8 is lower than for *dataset₁* and *dataset₃*, which suggests that the ML based indicator (but probably also the definition of accurate ground truth values by the expert) suffer from a growing number of pattern types.

4 Discussion and Conclusion

In summary, we presented a framework to design ML based indicators for process monitoring, which is able to integrate pattern recognition and ML methods. We showed that this framework is a generalization of the established control chart framework and therefore, directly extends classical process control approaches. We analyzed one application of the proposed setup in a case study, namely the Health Factor. Apart from demonstrating that the Health Factor fulfills the stated requirements, we evaluated its performance on 3 datasets from semiconductor industry and verified that the concept has not only theoretical, but also practical value.

Indicators, which fulfill the relaxed consistency condition are guaranteed to be reasonable from the viewpoint of human understanding, enabling that automated or semi-automated actions are taken. The proposed framework can simplify the transition from purely statistical key numbers to ML based approaches in practical applications, beyond the application in semiconductor industry. Adapting the concept to other industries is feasible, since the concept is exclusively dependent on the structure of the input data and expert knowledge (and not the source or format of the data). For instance, the framework can be applied to time series data, as well, if the feature extraction step is tailored. Instead of extracting properties from images, characteristics of time series, such as statistical moments, can be used for this purpose. Further, the flexibility to integrate challenging ML scenarios in the process monitoring framework, such as incremental learning [25] or the presence of unknown classes [23], is a strong benefit — however, further evaluations are necessary to extend the concept in such areas.

Integration of ML into automated or semi-automated systems and combining data-driven methods with domain and expert knowledge will most likely continue to be of high importance in the future, especially heading for fully automated manufacturing systems. Hence, our future work will consist of developing further ML based indicators based on the proposed concept aiming to bridge the gap between human know-how and computational exploitation of big data.

Acknowledgment

A part of the work has been performed in the project Power Semiconductor and Electronics Manufacturing 4.0 (SemI40), under grant agreement No 692466. The project is co-funded by grants from Austria (BMVIT-IKT der Zukunft, FFG

project no. 853338 and 6053321), Germany, Italy, France, Portugal and - Electronic Component Systems for European Leadership Joint Undertaking (ECSEL JU).

Further, a part of the work has been performed in the project Integrated Development 4.0 (iDev40). This project has received funding from the ECSEL Joint Undertaking (JU) under grant agreement No 783163. The JU receives support from the European Union's Horizon 2020 research and innovation programme and Austria (BMVIT-IKT der Zukunft, FFG project no. 865348 and 12248997), Germany, Belgium, Italy, Spain, Romania. The information and results set out in this publication are those of the authors and do not necessarily reflect the opinion of the ECSEL Joint Undertaking.

Further, a part of the work has been performed in the project Arrowhead Tools for Engineering of Digitalisation Solutions (Arrowhead Tools). This project has received funding from the ECSEL Joint Undertaking (JU) under grant agreement No 826452. The JU receives support from the European Union's Horizon 2020 research and innovation programme and Sweden, Austria, Spain, Poland, Germany, Italy, Czech Republic, Netherlands, Belgium, Latvia, Romania, France, Hungary, Portugal, Finland, Turkey, Norway, Switzerland.

References

- [1] W. A. Shewhart. *Economic Control of Quality of Manufactured Product*. D. Van Nostrand Company, Inc., New York, 1931.
- [2] S. Bersimis, S. Psarakis, and J. Panaretos. Multivariate statistical process control charts: an overview. *Quality and Reliability Engineering International*, 23(5):517–543, 2007.
- [3] Y. Liu, J. Zeng, J. Bao, and L. Xie. A unified probabilistic monitoring framework for multimode processes based on probabilistic linear discriminant analysis. *IEEE Transactions on Industrial Informatics*, 16(10):6291–6300, 2020.
- [4] S. Jin, F. Ye, Z. Zhang, K. Chakrabarty, and X. Gu. Efficient board-level functional fault diagnosis with missing syndromes. *IEEE Transactions on Computer-Aided Design of Integrated Circuits and Systems*, 35(6):985–998, 2015.
- [5] Z. Ge and Z. Song. Semiconductor manufacturing process monitoring based on adaptive substistical pca. *IEEE Transactions on Semiconductor Manufacturing*, 23(1):99–108, Feb 2010.
- [6] J. Yu. Semiconductor manufacturing process monitoring using gaussian mixture model and bayesian method with local and nonlocal information. *IEEE Transactions on Semiconductor Manufacturing*, 25(3):480–493, Aug 2012.
- [7] C. Aldrich and L. Auret. *Unsupervised Process Monitoring and Fault Diagnosis with Machine Learning Methods*. Springer, London, 2013.
- [8] T. Wuest, C. Irgens, and K.-D. Thoben. An approach to monitoring quality in manufacturing using supervised machine learning on product state data. *Journal of Intelligent Manufacturing*, 25(5):1167–1180, Oct 2014.
- [9] F. Lv, C. Wen, Z. Bao, and M. Liu. Fault diagnosis based on deep learning. In *2016 American Control Conference (ACC)*, pages 6851–6856, July 2016.
- [10] A. Angelopoulos, E. T. Michailidis, N. Nomikos, P. Trakadas, A. Hatziefremidis, S. Voliotis, and T. Zahariadis. Tackling faults in the industry 4.0 era—a survey of machine-learning solutions and key aspects. *Sensors*, 20(1):109, 2020.
- [11] Automotive Electronics Council. Guidelines for part average testing, Dec 2011.
- [12] S. Schrunner, A. Jenul, M. Scheiber, A. Zernig, A. Kaestner, and R. Kern. A health factor for process patterns - enhancing semiconductor manufacturing by pattern recognition in analog wafermaps. In *IEEE International Conference on Systems, Man and Cybernetics*, 2019. manuscript accepted for publication.
- [13] G. A. Susto, A. Schirru, S. Pampuri, S. McLoone, and A. Beghi. Machine learning for predictive maintenance: A multiple classifier approach. *IEEE Transactions on Industrial Informatics*, 11(3):812–820, Jun 2015.
- [14] Z. Shen and J. Yu. Wafer map defect recognition based on deep transfer learning. *2019 IEEE International Conference on Industrial Engineering and Engineering Management (IEEM)*, pages 1568–1572, 2019.
- [15] Y. Yuan-Fu. A deep learning model for identification of defect patterns in semiconductor wafer map. *2019 30th Annual SEMI Advanced Semiconductor Manufacturing Conference (ASMC)*, pages 1–6, 2019.
- [16] C. H. Jin, H. J. Na, M. Piao, G. Pok, and K. H. Ryu. A novel dbscan-based defect pattern detection and classification framework for wafer bin map. *IEEE Transactions on Semiconductor Manufacturing*, 32(3):286–292, 2019.

- [17] M. Saqlain, B. Jargalsaikhan, and J. Y. Lee. A voting ensemble classifier for wafer map defect patterns identification in semiconductor manufacturing. *IEEE Transactions on Semiconductor Manufacturing*, 32(2):171–182, 2019.
- [18] T. Santos, S. Schrunner, B. C. Geiger, O. Pfeiler, A. Zernig, A. Kaestner, and R. Kern. Feature extraction from analog wafermaps: A comparison of classical image processing and a deep generative model. *IEEE Transactions on Semiconductor Manufacturing*, 32(2):190–198, May 2019.
- [19] N. Dalal and B. Triggs. Histograms of oriented gradients for human detection. In *IEEE Computer Society Conference on Computer Vision and Pattern Recognition (CVPR'05)*, pages 886–893, June 2005.
- [20] R. Wang and N. Chen. Wafer map defect pattern recognition using rotation-invariant features. *IEEE Transactions on Semiconductor Manufacturing*, 32:596–604, 2019.
- [21] T. Nakazawa and D. V. Kulkarni. Anomaly detection and segmentation for wafer defect patterns using deep convolutional encoder–decoder neural network architectures in semiconductor manufacturing. *IEEE Transactions on Semiconductor Manufacturing*, 32(2):250–256, 2019.
- [22] J. Yu, X. Zheng, and J. Liu. Stacked convolutional sparse denoising auto-encoder for identification of defect patterns in semiconductor wafer map. *Comput. Ind.*, 109:121–133, 2019.
- [23] S. Schrunner, B. C. Geiger, A. Zernig, and R. Kern. A generative semi-supervised classifier for datasets with unknown classes. In *Proceedings of the 35th Annual ACM Symposium on Applied Computing, SAC '20*, page 1066–1074, New York, NY, USA, 2020. Association for Computing Machinery.
- [24] P. A. P. Moran. Notes on continuous stochastic phenomena. *Biometrika*, 37(1):17–23, Jun 1950.
- [25] Y. Kong and D. Ni. A semi-supervised and incremental modeling framework for wafer map classification. *IEEE Transactions on Semiconductor Manufacturing*, 33:62–71, 2020.